Development of Numerical Manifold Method and its Application in Rock Engineering

GUOWEI MA,* LEI HE AND XINMEI AN

School of Civil and Environmental Engineering, Nanyang Technological University, Singapore 639798.

1. Introduction

Rock mass is a natural geological material consisting of both continuous rock medium and discontinuous components such as joints, fractures, faults etc. To characterize the mechanical behaviors of such discontinuities in a computer model, either explicitly or implicitly, various numerical methods have been developed.

For problems where their characteristic length (defined by the smallest dimension of the problem) is much larger than their representative volume (i.e. the smallest volume over which a measurement can be made that will yield a value representative of the whole), the discontinuities can be implicitly modeled with a homogenization model to obtain the equivalent properties of the material which is heterogeneous and/or fractured. Continuum-based numerical methods such as the finite difference method (FDM), the finite element method (FEM), and the boundary element method (BEM) can be adopted to describe such problems.

However, for problems where the representative volume is either much larger than or of a similar order of the physical problem, the continuum hypothesis is violated and the explicit representation of discontinuities is desired. In FEM, various joint element or interface element models like 'Goodman joint element',[1] six-node fracture element,[2] joint element based on the theory of plasticity,[3] thin-layer element,[4] and interface element in contact mechanics[5] have been implemented. Despite these efforts, the treatment of fractures and fracture growth remains limited in the FEM. The FEM requires the finite element mesh conforming to the cracks, which complicates the meshing task. When fracture growth involved, remeshing is inevitable, which makes the simulation complicated and time-consuming. To overcome the inconveniences in meshing and remeshing processes, a variety of modifications to the conventional FEM have been made based on the partition of unity (PU). The extended finite element method (XFEM),[6,7] in which discontinuities and discontinuities in derivatives are directly represented by incorporating enrichment functions, and the generalized finite element mesh (GFEM),[8] which augments the finite element approximation space with high-order terms or handbook functions of boundary value problems to tackle some typical problems with multiple reentrant corners, voids, and cracks, are two representative examples.

Other continuum-based numerical methods for fracturing analysis include the BEM and the meshless methods. In general, the BEM is not efficient as the FEM in dealing with material heterogeneity and non-linearity. Meshless methods look promising, but are not sufficient to replace the FEM because of their difficulties in numerical integration of weak forms and imposition of essential boundary conditions.

The continuum-based numerical methods can deal with the fractures to some extent. Block rotations, complete detachment and large-scale opening can not be treated.

Discontinuum-based numerical methods including the distinct element method (DEM) originated by Cundall[9] and the discontinuous deformation analysis (DDA) method pioneered by Shi[10] are also used in modeling the rock mass behaviors. In these methods, the

*Corresponding author. E-mail: CGWMa@ntu.edu.sg

Analysis of Discontinuous Deformation: New Developments and Applications.
Edited by Guowei MA and Yingxin ZHOU. *Published by* Research Publishing Services.

ISBN: 978-981-08-4455-4
doi:10.3850/9789810844554-keynote-Ma-Guowei

problem domain is treated as an assemblage of rigid or deformable blocks with the contacts between them identified and continuously updated during the entire deformation/motion process. This kind of methods is especially suitable for the simulation of large-scale displacements of individual blocks, block rotations, and complete detachment.

It is often the case that individual discrete blocks can also fracture or fragment, which is in essence a process of transition from continua to discontinua. Such problems can be well represented by the combined continuum-based and discontinuum-based numerical methods, such as the combined finite-discrete element method[11] and the numerical manifold method (NMM).[12]

The NMM was initially proposed by Shi in 1991. It gains her name after the mathematical notion of manifold.

Different from other numerical approaches, the NMM adopts a finite number of small patches called covers to discretize the problem domain, defines local approximations called cover functions on each cover, and uses weight functions (or partition of unity functions) to paste the local approximations together to give a global approximation.

Compared with other numerical methods, the NMM has the following three distinct features: (1) because of the introduction of covers, the discontinuities are treated in a straightforward manner; continuous body, fractured body, and assemblage of discrete bodies are treated in a unified form; (2) the covers do not need to conform to neither the external boundaries nor the internal features such as cracks and material interfaces, which makes its preprocessing easy and discontinuity evolutions be modeled without remeshing; (3) because of the partition of unity property of its weight functions, high-order terms or special functions can be easily incorporated into its local approximations to improve the accuracy.

In this paper, firstly, the basic theories of the NMM are briefly introduced Then some applications of the 2D-NMM, including the modeling of multiple discrete blocks, the modeling of strong discontinuities, and the 3D-NMM, including 3D block cutting, the displacement and deformation modeling, are presented, respectively.

2. Basic Theory of the NMM

2.1. *NMM components*

With reference to an example in Fig. 1, the definitions of three basic components in the NMM, namely the mathematical cover (MC), the physical cover (PC) and the cover based manifold element (CE), are presented.

The portrait of the physical problem including the problem domain in which the physical problem is defined, and all the physical features such as the internal discontinuities (e.g. cracks, joints, material interfaces, holes, etc.) and the external geometries on which boundary conditions are prescribed is referred to as a physical domain (Fig. 1(a)), whereas a domain which is independent but completely cover the physical domain is called the mathematical domain (Fig. 1(b)).

The mathematical domain can be constructed as a union of a finite number of small patches, called mathematical covers, denoted as MC_I. The mathematical covers are user-defined, can be of arbitrary shape and can overlap each other partially or completely. They are defined completely independent of the physical domain. However, their union must be large enough to cover the entire physical domain. See the example in Fig. 1, there are two mathematical covers in total, denoted as MC_1 and MC_2 (Fig. 1(c)).

The physical covers are the intersection of mathematical covers and the physical domain. If completely cut by the physical features, a mathematical cover MC_I will be partitioned into

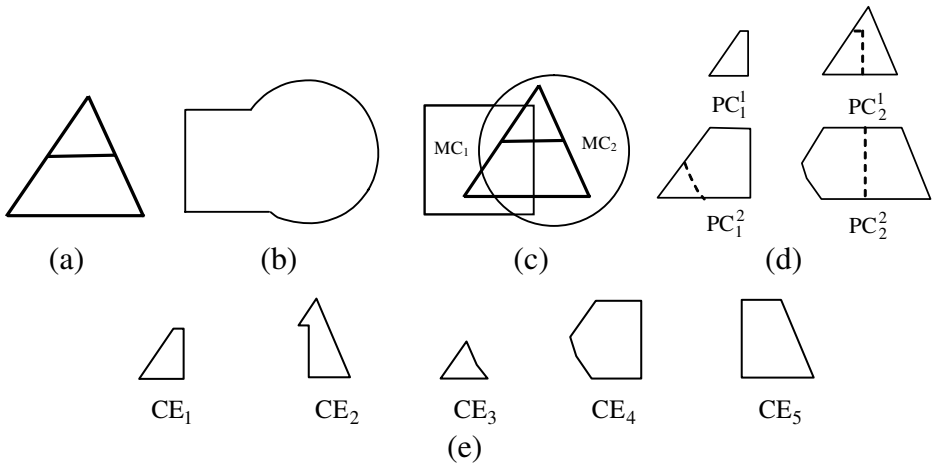

Figure 1. NMM components in 2D-NMM: (a) physical domain; (b) mathematical domain; (c) mathematical covers; (d) physical covers; (e) cover-based manifold elements.

several physical covers, denoted as $\mathrm{PC}_I^j (j = 1 \sim m_I)$. See the example in Fig. 1, mathematical cover MC_1 is completely cut into three isolated regions by the physical features and two of them are within the problem domain, so two physical covers, denoted as PC_1^1 and PC_1^2 are formed (Fig. 1(d)). Similarly, mathematical cover MC_2 also forms two physical covers, denoted as PC_2^1 and PC_2^2.

The cover-based manifold element is defined as the common region shared by several physical covers. The four physical covers in Fig. 1(d) finally form five cover-based manifold elements, shown in Fig. 1(e).

Figure 2(a) illustrates the three basic components of the 3D-NMM. There are two mathematical covers in total, i.e. a sphere mathematical cover MC_1 and a hexahedron mathematical cover MC_2. The pyramid defines the physical domain. Intersected with the physical domain, two physical covers i.e. PC_1^1 and PC_2^1 as shown in Fig. 2(b) are generated. These two physical covers finally form three cover-based manifold elements, as shown in Fig. 2(c).

2.2. *NMM approximations*

On each mathematical cover MC_I, a weight function $\varphi_I(x)$ satisfies

$$\begin{aligned} &\varphi_I(x) \in C^0(\mathrm{MC}_I) \\ &\varphi_I(x) = 0,\ x \notin \mathrm{MC}_I \end{aligned} \tag{1a}$$

$$\sum_{\substack{K \\ if\ x \in \mathrm{MC}_K}} \varphi_K(x) = 1. \tag{1b}$$

Equation (1a) indicates that a weight function $\varphi_I(x)$ is continuous over the mathematical cover MC_I, and has non-zero value only on its corresponding mathematical cover MC_I, but zero elsewhere, whereas Eq. (1b) is known as the partition of unity (PU) for the continuity of approximation.

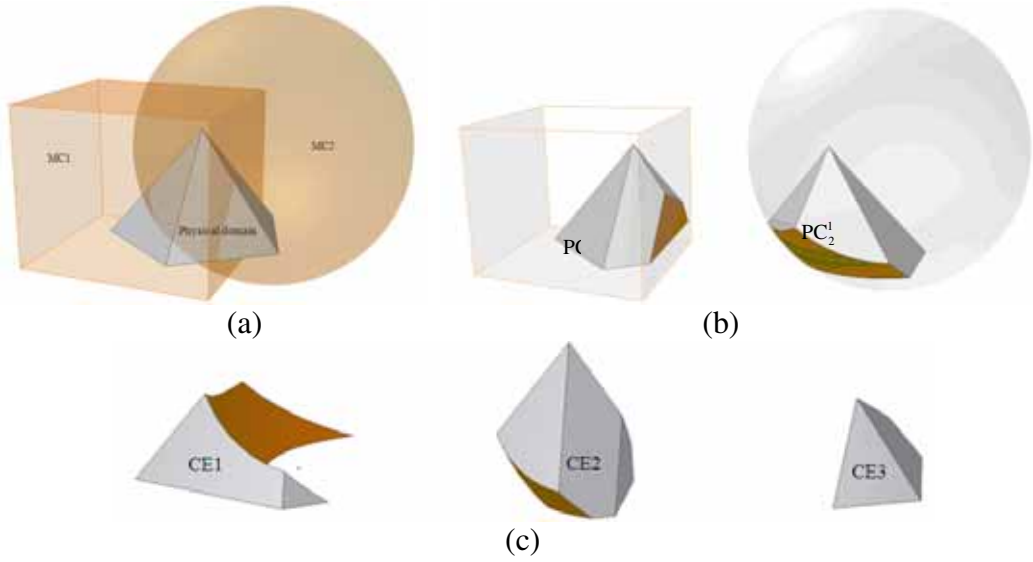

Figure 2. NMM components in 3D-NMM: (a) physical domain and mathematical covers; (b) physical covers; (c) cover-based manifold elements.

On each physical cover PC_I^j, a local approximation function called cover function denoted as $u_I^j(x)$ is defined. Weight functions defined on each mathematical cover transfer to the physical covers as

$$\varphi_I^j(x) = \delta_I^j \cdot \varphi_I(x) \tag{2}$$

where δ_I^j is a modifier, with its value to 1 within the physical cover PC_I^j and 0 elsewhere. Here, each physical cover has two indices, I and j. To simplify the implementation, we reallocate a single index i to each physical cover with i gained by

$$i(I,j) = \sum_{l=1}^{I-1} m_l + j \tag{3}$$

Thus, physical cover PC_I^j, cover function $u_I^j(x)$ and weight function $\varphi_I^j(x)$ are re-denoted as PC_i, $u_i(x)$ and $\varphi_i(x)$, respectively. Then, we use the weight functions $\varphi_i(x)$ to paste all the cover functions $u_i(x)$ together to give a global approximation over each cover-based manifold element as

$$u^h(x) = \sum_{\substack{i \\ \text{if CE} \subset P_i}} \varphi_i(x) \cdot u_i(x) \tag{4}$$

Because of the partition of unity property of the weight functions, any high-order terms or special functions can be incorporated into the cover functions to give a high-accuracy approximation.

2.3. *Imposition of essential boundary condition*

In the NMM, the mathematical covers are constructed totally independent of the boundaries. The essential boundary condition thus can not be accomplished by directly enforcing the degrees of freedom like in the FEM, but is usually prescribed by the Lagrange multiplier method, the penalty method or the augmented Lagrange multiplier method in the weak form of governing equations.[13]

2.4. *Contact problems in the NMM*

The NMM aims at solving the discontinuous problems, even with rigid movements. When intersected with physical features like weak discontinuities and strong discontinuities, each mathematical cover forms several independent physical covers associated with individual cover functions. So, the adjacent cover-based manifold elements formed by these physical covers are independent on each other in the framework of the NMM.

However, the fact is that the cover-based manifold elements at the two sides of the discontinuities are not totally independent, but have some relations. For example, for a problem domain containing a strong discontinuity, the displacement field across the crack surface is discontinuous; however, the two sides, i.e. upper side and lower side, of a crack surface can not penetrate each other in geometry even under a complex stress state. Another example is the problem with discrete bodies. The displacement field across each body boundary is discontinuous; however, one body can not penetrate into another body Such constraints are normally termed non-penetration or unilateral condition, and attributed to a contact problem in physics.

Since the frictional contact problems are inherently nonlinear and irreversible, for the sake of generality, an incremental approach is adopted in the NMM. The contact state at the beginning of the current time step is known and the contact state at the end of the current step after a time interval of step time is to be solved, while the time incremental for each time step is chosen small enough so that the displacements of all the points within the problem domain are less than a predefined maximum displacement limit ρ. With an open-close iteration procedure, the contact constraint of no penetration and no tension of the two sides of discontinuous entities are fulfilled. Detailed contact detection and modeling in the 2D-NMM can refer to Shi.[12]

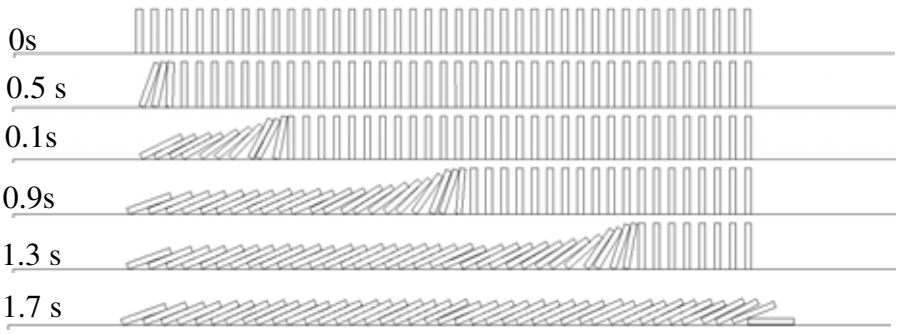

Figure 3. Toppling process of a series of blocks modeled by the NMM.

3. Applications of the 2D-NMM

3.1. *Modeling of multiple discrete blocks*

The problems with multiple discrete bodies which are described well with the DDA can also be modeled with the NMM. A typical domino run problem is numerically investigated here. The numerical model consists totally 41 rectangular blocks with the size of 20 mm×150 mm and the spacing of 30 mm on a horizontal surface. The material parameters for the blocks are: Young's modulus $E = 200\,\text{GPa}$, Poisson's ration $\nu = 0.3$. The fiction coefficient μ between the blocks and the horizontal surface is 0.3. An initial pulse force is applied to the first block to make it topple to the second block, which induce a toppling process shown in Fig. 3. The numerically obtained result is consistent with the experimentally observed phenomenon.

Another example is the NMM modeling of mineral separation process using the vibrating screen. The simplified model includes a set of coal blocks, a vibrating screen and a container. The screen moves in the horizontal direction with a frequency of 1 Hz and amplitude of 5.5 cm.

In the study, an oversize triangle is used to cover the whole problem domain, which treats each block as a single cover-based manifold element with constant stress field and linear displacement field. It is reasonable because the coal blocks generally undergo small deformation during the separation process. The numerically obtained separation process is shown in Fig. 4.

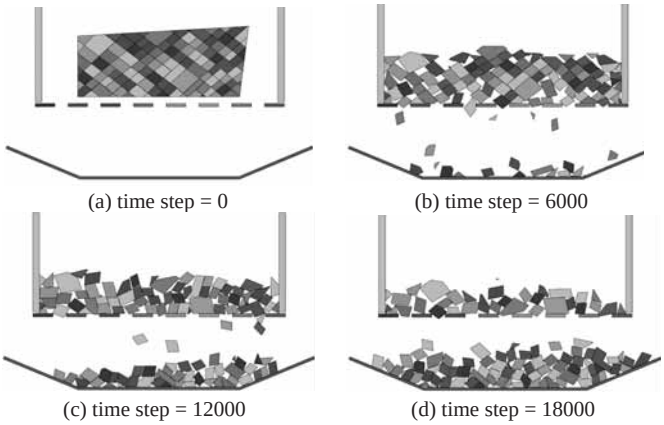

Figure 4. Size separation process with the vibrating screen modeled by the NMM.

3.2. *Modeling strong discontinuities*

The NMM models the strong discontinuities by splitting mathematical covers completely cut by the crack surfaces into several physical covers attached with independent cover functions and enriching singular physical covers containing the crack tips with asymptotic crack tip functions.[14,15] The resulting displacement field across discontinuities is naturally discontinuous. The NMM models complex cracks in an exactly same way with the modeling of a single crack.

Numerical examples in Refs. 14 and 15 have demonstrated the efficiency and robustness of the NMM in modeling complex cracks and their growth. For illustration purpose, a problem with a tree-shaped crack under bi-axial tension in a finite plate shown in Fig. 5(a) is examined here. The detailed description of the parameters used in the computation can refer to Ref. [14]. The regular mathematical covers for the central part of the problem are depicted in Fig. 5(b). The convergence of the stress intensity factors (SIFs) at crack tip D can be easily observed when the mathematical covers are gradually refined (Fig. 5(c)).

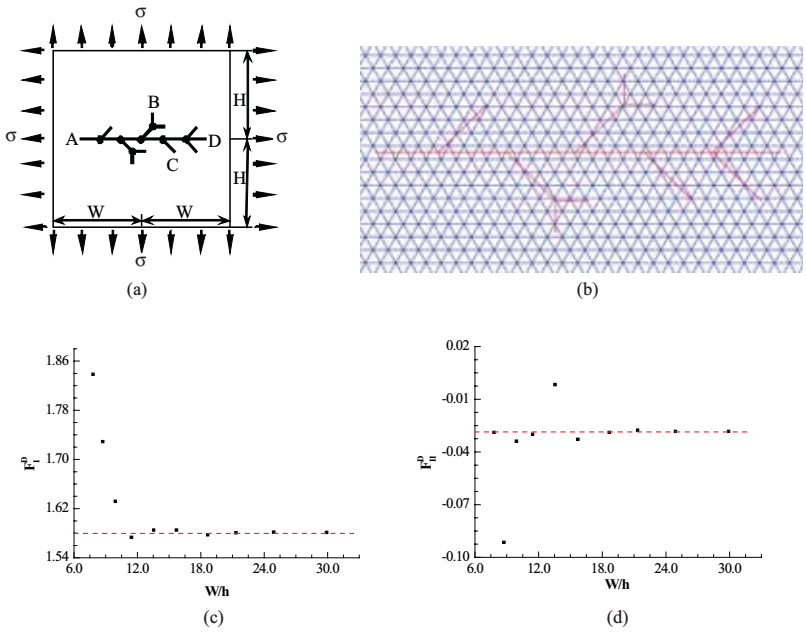

Figure 5. Modeling a tree-shaped crack with the NMM: (a) a problem with a tree-shaped crack; (b) part of the mathematical covers; (c) SIFs at crack tip D.

4. Applications of the 3D-NMM

4.1. *Block cutting*

A cutting algorithm[16] is proposed to generate blocks from joints and free faces in a three-dimensional space.

If the joints are long compared with the dimension of the target block, cutting algorithm is simple. Only convex blocks are generated. However, if the joints are shorter than the dimension of the target block, the cutting algorithm becomes complicated because: (1) the blocks may be concave; (2) the faces of the blocks may be concave; (3) a block may contain sub-blocks inside; (4) a block may contains holes inside; (5) the faces of blocks may also contains sub-faces or holes inside.

Most existing block cutting codes only deal with the cases in which the joints are long enough to cut through the target block and thus produce only convex blocks. However, our

proposed algorithm can describe not only convex blocks but also concave blocks, not only simply connected blocks but also multiply connected blocks.

Figure 6(a) depicts the Great Pyramid of Khufu with internal chambers, while Fig. 6(b) illustrates our 3D cutting result, which is a convex block with complex internal faces. Figure 7 illustrates the cutting of a complex tunnel system in a jointed rock mass. Figure 8 shows the cutting of a slope in a jointed rock mass.

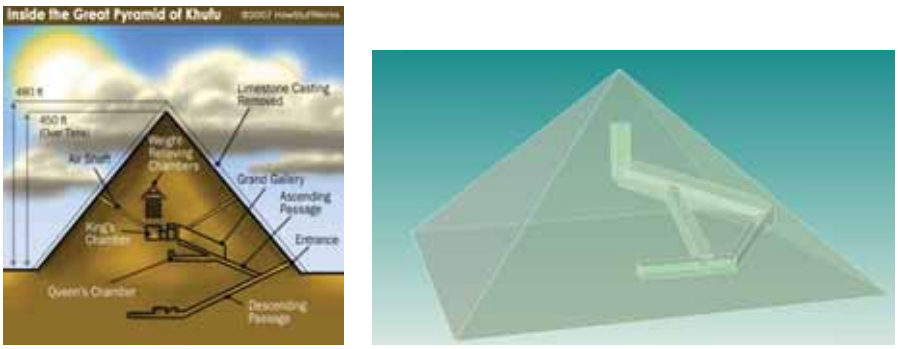

(a) (b)

Figure 6. Cutting the Great Pyramid of Khufu: (a) real structure; (b) 3D cutting result.

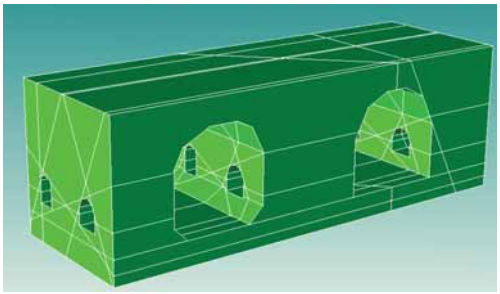

Figure 7. Cutting a tunnel system in a jointed rock mass.

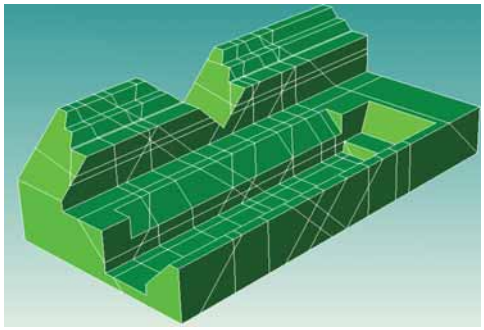

Figure 8. Cutting a slope in a jointed rock mass.

4.2. *Modeling of block free fall*

In Fig. 9(a), the geometry of a single block in the 3-D space can be defined by using the explanation of physical covers and mathematical covers mentioned in the previous sections. The cube falls under the pure influence of the gravity. The acceleration of gravity is 10 m/s^2. The time step used is 0.05 s.

Figure 9(b) gives the displacement time history. The error of the numerical solution is less than 0.1% in the maximum absolute difference, which illustrates the accuracy of the NMM calculation.

4.3. *Effect of cover size and orientation*

A 2 m×2 m×0.1 m plate is subjected to the gravity load with $g = 10$ and fixed at four corners, with material properties of $E = 10$ GPa, $\nu = 0.3$, $\rho = 1200$ kg/m^3. Its geometry of typical mesh design is shown in Fig. 8(a) in which faces of the plate conform to the axis planes.

Six mathematical cover size of $s = 0.52$, 0.32 0.22, 0.12, 0.08, 0.05 are used to examine the cover size effect. After intersection with the physical plate, 190, 684, 1104, 3706, 8100, 19200 cover-based manifold elements are generated respectively. The dynamical ratio is set

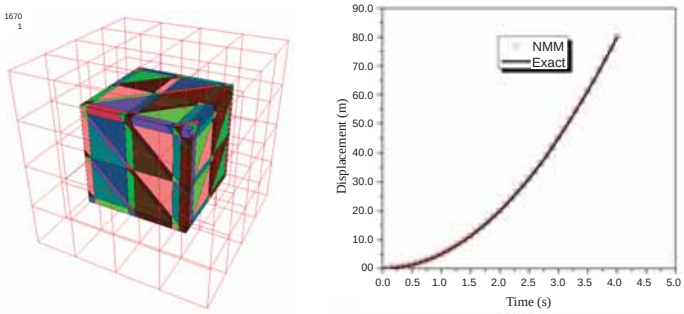

(a) (b)

Figure 9. Block free fall simulation: (a) the model; (b) the displacement time history versus theoretical solution.

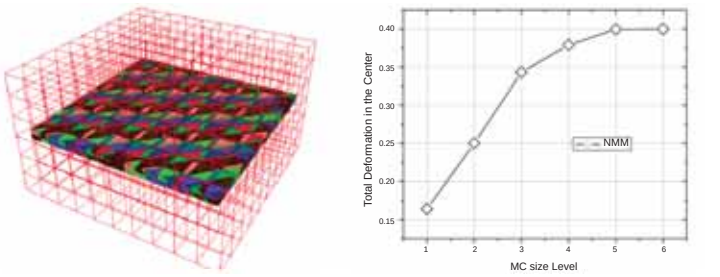

(a) Model (b) Convergence of deformatiom

Figure 10. Deformation convergence with decrease of cover size.

to be 0 to clarify the quasi-static responses of the 6 models. Hence, no velocity of the cover-based manifold element is transferred to the next time step. Results are convergent and stable with the increase of the mesh density shown in Fig. 10(b).

Then, the 2 m×2 m×0.1 m plate is subjected to a constant point load $L = 5$ at the center with fixed four corners of the same material properties above. The dynamical ratio is set as 0.999 to investigate dynamical response fully. Two different orientations of the plate (orientation 2 and 3) are shown in Fig. 11 where the orientation 1 is same as the previous example.

Z direction displacement histories of the center point (Fig. 12) shows that the orientation of the mathematical covers has negligible effect on the plate maximum displacement at the plate center. The maximum displacement is accurate and stable after converging, and the convergence time is also stable.

This ensures the accuracy and modeling efficiency of the 3-D NMM and decreases the mesh division complexity in FEM. It also supports the validity of the 3-D NMM dynamic algorithm.

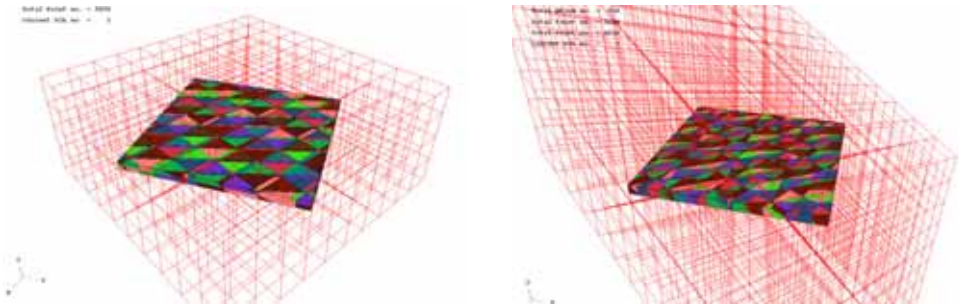

Figure 11. Geometry of mesh designs for mesh orientation effect study.

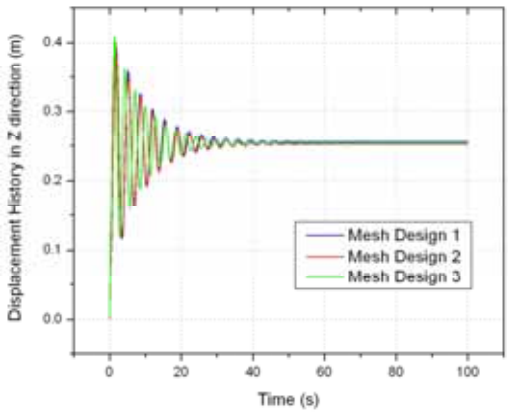

Figure 12. Z direction displacement histories of center point.

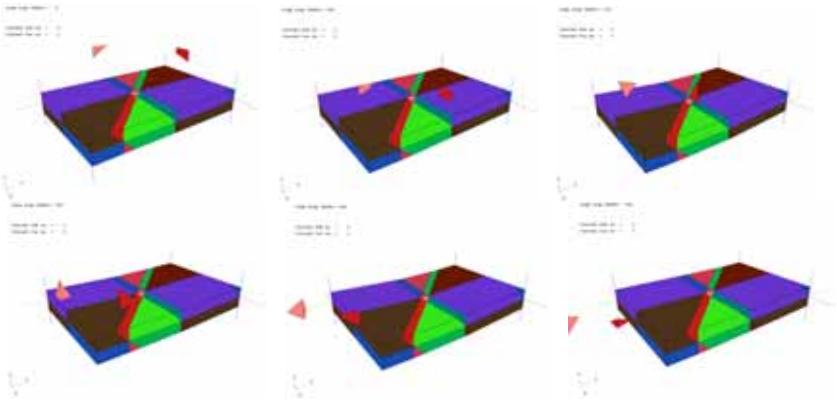

Figure 13. two tetrahedron contact with flexible slab.

4.4. *Contact algorithm*

As shown in the Fig. 13 a flexible slab has been fixed on three corners, and one corner is free. Two tetrahedron blocks are suspending above the slab. The whole system is under gravity environment and equivalent 0.4 gravity force along minus y direction

In recent developing NMM 3D code, contact system built upon contact hierarchies' concept (HTC), which has been used in the commercial software LSDYNA. It is one of most confidential contact algorithm recently. Furthermore, NMM3D formula can simulate the whole dynamical process, such as fell down, contact interaction, frictional sliding, and separation

This algorithm is still under optimization. Up until now, the advantage of this algorithm in discontinuous description and contact interaction, has facilitated and provided foundation for its wide usage in complex underground engineering.

5. Conclusions and Remarks

In the NMM, two separate cover systems i.e. the mathematical covers and the physical covers are employed to describe a physical problem with displacement approximations defined on each physical cover. The displacement approximation on a coverbased manifold element is obtained by the combination of the approximations of the related physical covers using the partition of unity. As elements across discontinuous entities may be related with different physical covers, the NMM can describe continuous problems and discontinuous problems simultaneously in a unified form. By increasing physical covers, the process from continua to discontinua can be easily actualized without any difficulties that are encountered in other numerical methods Obviously, the NMM is a promising numerical method in many research and application areas, and the rock mechanics and rock engineering area is certainly and importantly included

In this paper, focus is put on the development and verifications of both the 2D-NMM and 3D-NMM. As the basic theory of the 2D-NMM has developed relatively well, it is used to simulate discrete block systems and developed for crack simulation. Results show that the 2D-NMM can deal with discrete and strong discontinuous problems well. Fundamental studies are carried out for the 3D-NMM, including block cutting and the application of 3D-NMM in both continuous and discontinuous problems. The satisfied verification results of the 3D-MM program put a solid stage for its further development.

References

1. Goodman R. E., Taylor R. L., Brekke T. L. A model for the mechanics of jointed rock. *Journal of the Soil Mechanics and Foundations Division*, ASCE, 1968, 94: 637–659.
2. Zienkiewicz O. C., Best B., Dullage C., Stagg K. Analysis of nonlinear problems in rock mechanics with particular reference to jointed rock systems. *Proceedings of the Second International Congress on Rock Mechanics*, Belgrade, 1970, pp. 8–14.
3. Ghaboussi J., Wilson E.L, Isenberg J. Finite element for rock joints and interfaces. *Journal of the Soil Mechanics and Foundations*, ASCE, 1973, 99(10): 849–862.
4. Desai C. S., Zamman M. M., Lightner J. G., Siriwardane H. J. Thinlayer element for interfaces and joints. *International Journal for Numerical and Analytical Methods in Geomechanics*, 1984, 8: 19–43.
5. Katona M. G. A simple contact–friction interface element with applications to buried culverts. *International Journal* for *Numerical* and Analytical *Methods* in *Geomechanics*, 1983, **7**: 371–384.
6. Moes N., Dolbow J., Belytschko T. A finite element method for crack growth without remeshing. *International Journal for Numerical Methods in Engineering*, 1999, 46: 131–150.
7. Sukumar N., Prevost J. H. Modeling quasi-static crack growth with the extended finite element method Part I: computer implementation. *International Journal of Solids and Structures*, 2003, 40: 7513–7537.
8. Strouboulis T., Babuska I., Copps K. The design and analysis of the generalized finite element method, *Computer Methods in Applied Mechanics and Engineering*, 2000, 181: 43–69.
9. Cundall P. A. A computer model for simulating progressive, large scale movements in blocky rock systems, *Proceedings, International Symposium on Rock Fracture*, Nancy, France, II-8, 1971
10. Shi G. H. Discontinuous Deformation Analysis — A new numerical model for the static and dynamics of block systems, PhD Dissertation, Department of Civil Engineering, U.C. Berkeley, 1988
11. Munjiza A. The combined finite-discrete element method, Wiley, Chichester, 2004
12. Shi G. H. Manifold method of material analysis, *Trans. 9th Army Conf. on Applied Mathematics and Computing*, Minneapolis, Minnesota, 1991, pp. 57–76.
13. Ma G. W., An X. M., He L. The numerical manifold method-A reivew. Submitted to *International Journal of Computational Methods*, 2009.
14. Ma G. W., An X. M., Zhang H. H., Li L. X. Modeling complex crack problems with numerical manifold method. *International Journal of Fracture*, 2009 156 (1): 21–35.
15. Zhang H. H., Li L. X., An X. M., Ma G. W. Numerical analysis of 2-D crack propagation problems using the numerical manifold method. Submitted to *Engineering Analysis with Boundary Elements*, 2009.
16. Ma G. W., He L. Development of 3-D numerical manifold method. Submitted to *International Journal of Computational Methods*, 2009